Optimisation of a multiphase intermetallic metal–metal composite material

J. D. Robson, N. Duvauchelle, A. Lugan, J. Street, and H. K. D. H. Bhadeshia

Metal–metal composites (MeMeCs) manufactured by coextruding β[Ni(Al,Ti)], β'[Ni_2AlTi] and γ'[Ni_3(Al,Ti)] show promise as high strength, heat resistant materials. The best combination of strength and plasticity are obtained by using a high fraction (0·8) of γ' as the matrix phase combined with equal fractions of β and β' reinforcement. Further improvements in properties may be obtained by increasing the fracture strength of the matrix phase following the methods used in monolithic γ' alloys. Boron additions are shown to lead to significant improvements in tensile fracture strength. The highest levels of plasticity were obtained in an MeMeC material which had a matrix composition designed to allow the more ductile γ phase to precipitate in the γ', as well as containing boron to increase grain boundary cohesion. Fractography suggests that tensile failure occurs in this material in a much more ductile way, with evidence of local plastic deformation and a largely transgranular failure mode rather than the intergranular fracture observed in the other MeMeC materials. **MST/4711**

At the time the work was carried out the authors were in the Department of Materials Science and Metallurgy, University of Cambridge, Pembroke Street, Cambridge CB2 3QZ, UK. Dr Robson is now in the Manchester Materials Centre, Grosvenor Street, Manchester M1 7HS, UK (joseph.robson@umist.ac.uk). *Manuscript received 31 May 2000; accepted 7 August 2000.*

Introduction

Single phase intermetallic materials, while often possessing desirable properties such as low density and good oxidation resistance, are often limited in their application either by poor low temperature ductility or inadequate elevated temperature strength. Many efforts have therefore focused on the development of multiphase intermetallic materials, with the complementary phases used either to enhance strength or ductility. Such materials may be produced by solid state precipitation and directional solidification.[1–4] Another possibility which allows greater control over the final microstructure than obtained with solid state precipitation is to mechanically combine the individual constituent phases in the required proportions. This approach was used by Hsuing and Bhadeshia[5] and Robson and Bhadeshia[6] to produce three phase β[Ni(Al,Ti)]–β'[Ni_2AlTi]–γ'[Ni_3(Al,Ti)] materials which they referred to as metal–metal composites (MeMeCs). In these materials the strong but brittle β and β' phases act as reinforcement in a matrix of the more ductile γ' phase.

In both studies, the γ, β, and β' were manufactured independently in powder form. The powders were then coextruded to give the required intimate dispersion of the three phases in the final material. The chemical compositions of the γ, β, and β' powders had been chosen to correspond to the corners of a tie triangle defining the three phase equilibrium at 900°C. This ensured the high temperature stability of the microstructure following consolidation. It was discovered that this method could be used successfully to produce a thermally stable multiphase intermetallic material which exhibited good compressive strength levels, coupled with significant plasticity before failure.[5] By refining the size of the powders and optimising the extrusion conditions further improvements in compressive failure strain were achieved.[6] Nevertheless, failure in compression still occurred after relatively low plastic deformation ($\sim$11% at room temperature). Studies of failed specimens showed that the grain boundaries in the γ' phase were a source of weakness. Furthermore, the tensile properties of the MeMeC materials are yet to be characterised. The aim of the present work was to modify the compositions of the starting phases in an attempt to improve ductility, as well as determine the tensile properties of the MeMeC material.

Method

MODIFIED COMPOSITIONS

Previous work demonstrated that MeMeC material with a high proportion of γ' phase ($80\gamma'-10\beta-10\beta'$, wt-%) shows the best compressive strain to failure without significant loss of strength when compared with MeMeC variants with higher levels of β and β' (Refs. 5 and 6). In compression, MeMeC has been shown to fail by the propagation of cracks which initiate in the brittle β and β' phases or at the interphase boundaries. Although the γ' matrix offers more resistance to crack propagation than the β or β', cracks nevertheless occur along grain boundaries in this phase. These link up and lead to general failure.

There probably is little scope for increasing greatly the crack resistance of the β and β' phases.[7,8] However, the ductility may be increased by enhancing the resistance of the matrix γ' to transgranular crack propagation. In the present study, modifications were made to the matrix phase composition to achieve this.

It is well established that boron additions to polycrystalline γ' phase can enhance its tensile ductility.[9] Boron segregates to the grain boundaries where it is thought to enhance the cohesion of atoms, thereby inhibiting intergranular cracking. It is also well known that this effect works only for γ' alloys which are on the nickel rich side of the stoichiometric Ni_3(Al,Ti) composition; i.e. the γ' should contain more than 75 at.-%Ni for the boron to be effective. One aim of the present investigation was to determine whether the boron effect can be exploited successfully for MeMeC, and what effect this would have on strength and ductility.

The compositions of the powders used in the original work were chosen to coincide with the three corners of the $\beta-\beta'-\gamma'$ tie triangle on the isothermal section at 900°C, of the ternary phase diagram (Fig. 1).[10] The position of this tie triangle does not change much with temperature and thus there should be little tendency for dissolution or re-precipitation of any of the three phases up to this

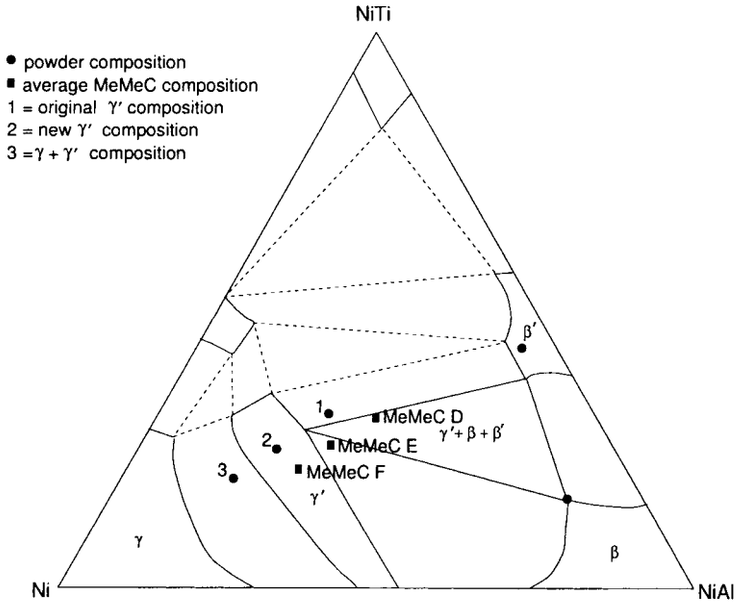

1 Nickel rich corner of ternary Ni–Al–Ti phase diagram at 900°C (after Ref. 10) showing compositions of powders used in present investigation and average composition of MeMeC variants

temperature. The three original powder compositions are shown in Table 1. It can be seen that the nickel concentration in the original γ' powder is below the critical level required for boron additions to be effective. New γ' powder was therefore manufactured with a nickel level of 76 at.-%, in excess of the stoichiometric concentration (Table 1). Both boron doped (0·1 wt-%B) and boron free variants of this powder were produced.

Another possible method for ductilising the matrix phase is by designing its composition so that it contains a small fraction of the disordered, more ductile γ phase as well as γ'. To investigate this, two more powders were manufactured with compositions which lay in the two phase $\gamma+\gamma'$ region on the phase diagram (Fig. 1). One of these powders was doped with boron to investigate the combination of both effects.

MeMeC FABRICATION

The powders were manufactured following the same methodology as in previous investigations.[6] The β and β' powders were prepared by mechanically crushing cast ingots. All the other powders were prepared by argon gas atomisation. The mean particle sizes of the new γ' and $\gamma+\gamma'$ powders were similar to those of the original γ' powder (with diameter approximately equal to 70 μm). X-ray diffraction studies of each powder were performed using a diffractometer with Cu K_α (doublet $\lambda=1{\cdot}5406$ and 1·54439 Å) radiation to determine which phases were present. The powders were then blended together in the proportions used in previous work ($10\beta-10\beta'-80(\gamma'$ or $\gamma+\gamma'$), wt-%) and mixed using a small mechanical mill.

Extrusion was carried out at Inco Alloys UK using the following procedure: the blended powder was sealed in an Incoloy 800 alloy can, preheated to 1170°C for 2 h and then extruded using a 16 : 1 reduction ratio, a ram speed of 25 mm s^{-1}, and two layers of C glass as lubricant. Table 2 summarises the nomenclature used to identify varieties of samples manufactured in this and previous studies.

Table 1 Measured compositions of nominally single or two phase alloy powder (in at.-%) used to manufacture MeMeC: composition corresponding to corners of equilibrium tie triangle are given in parentheses

Phase	Ni	Al	Ti	B
γ' old	70·8 (72·7)	13·5 (12·9)	15·7 (14·4)	…
β old	56·1 (56·5)	36·3 (35·9)	7·6 (7·6)	…
β' old	52·7 (53·2)	25·8 (25·1)	21·5 (21·7)	…
γ' new	76·4	11·0	12·5	…
γ' new (with B)	76·4	11·0	12·5	0·03
$\gamma+\gamma'$	81·4	8·8	9·7	…
$\gamma+\gamma'$ (with B)	81·4	8·8	9·7	0·03

MICROSCOPY AND MECHANICAL TESTING

Following extrusion, specimens were polished and etched with Kalling's solution (2 g $CuCl_2$, 40 mL HCl, 50 mL ethanol) for optical examination. Compression test specimens were prepared by cutting rectangular blocks $2{\cdot}5\times2{\cdot}5\times6{\cdot}0$ mm from the extruded bar in either a longitudinal or transverse orientation using an SiC slitting wheel. Before testing the surface of the specimens was lightly ground using 1200 grit SiC paper. Compression testing was performed using a 50 kN servohydraulic testing machine. Specimens for elevated temperature testing were allowed thermal expansion under a small constant load and were held for 30 min at the testing temperature to ensure thermal equilibrium had been achieved within the furnace. Tests were carried out at temperatures up to 800°C, with each test repeated at least three times. The strain rate for all tests was about $2{\cdot}3\times10^{-4}$ s^{-1}.

Table 2 Metal–metal composite materials which have been manufactured to date: subscript 'o' refers to old powders and 'n' to new powders

MeMeC	β, %	β', %	γ'_o, %	γ'_n, %	$[\gamma'_n+B]$, %	$(\gamma+\gamma')_n$, %	$[(\gamma+\gamma')_n+B]$, %
B*	25	25	50	…	…	…	…
C*	15	15	70	…	…	…	…
D†	10	10	80	…	…	…	…
E	10	10	…	80	…	…	…
E_B	10	10	…	…	80	…	…
F	10	10	…	…	…	80	…
F_B	10	10	…	…	…	…	80

*Investigated by Hsuing and Bhadeshia.[5]
†Investigated by Robson and Bhadeshia.[6]

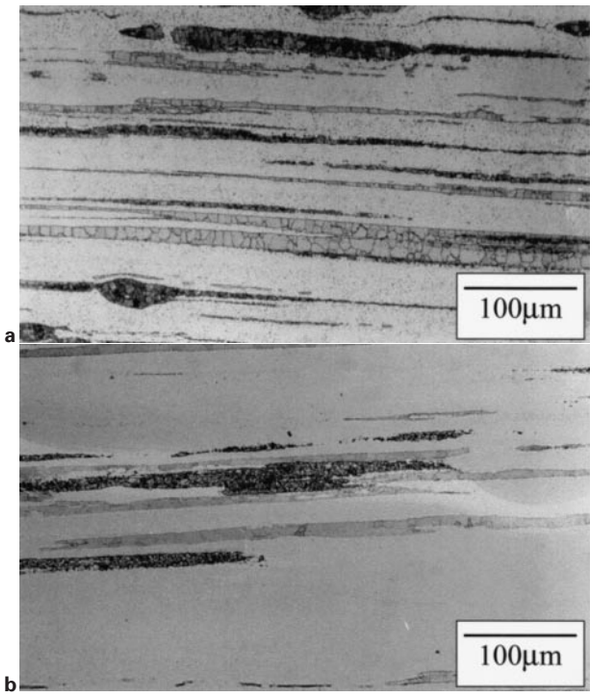

a MeMeC E; *b* MeMeC F

2 Optical micrographs of given specimen types in longitudinal direction: β' phase appears dark grey, β is lighter grey, and both γ and γ' appear almost white

Standard cylindrical threaded Rolls-Royce RLH10186 tensile specimens were manufactured by P S Marsden, UK using cylindrical grinding. The screw threads at the ends of the specimen were also manufactured by grinding as the hard and relatively brittle nature of the MeMeC material prohibited the use of more common methods. The specimen axis was in all cases parallel to the extrusion direction. Tensile testing was performed at room temperature using a 100 kN servohydraulic testing machine. Three tests were performed for each MeMeC variant. Following testing, scanning electron microscopy (SEM) was used to examine the fracture surfaces of the failed specimens.

Results

POWDER COMPOSITIONS

X-ray diffraction patterns of the γ' and $\gamma+\gamma'$ powders confirmed the absence of unexpected phases. The original γ' powder, used in previous work, had contained measurable quantities of β' and the hexagonal close packed η phase (Ni_3Ti). These phases were not detected in the new powders.

The presence of γ in the nominally $\gamma+\gamma'$ powder can be inferred from the intensity ratio of selected reflections. The face centred cubic (fcc) γ phase will only contribute to the diffracted intensity when h, k, and l are either all odd or all even. The intensity of the γ' superlattice reflections (h, k, l mixed odd and even) relative to that of the fcc lattice reflections will thus be reduced by the presence of the γ phase. The ratios of intensities of the (100) and (110) superlattice reflections to that of the (200) reflection are shown in Table 3. The (200) reflection was taken as the reference as it does not overlap with any β or β' reflections. The intensity ratio of the superlattice reflections is significantly lower in the nominally two phase $\gamma+\gamma'$ powder than the γ' powder, suggesting that γ is indeed present.

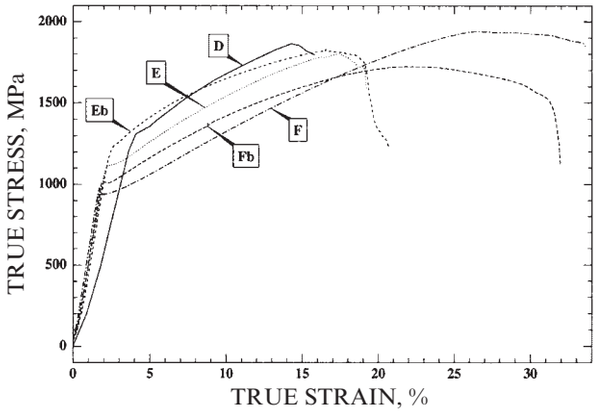

3 Typical room temperature true stress *v.* true strain curves (in compression in transverse direction) for MeMeC D, E, E_B, F, and F_B

AS EXTRUDED MeMeC

Optical micrographs of MeMeC E and F are shown in Fig. 2. A fibrous, intimate dispersion of the β, β', and matrix phases is observed as expected. It is not possible to differentiate between the γ and γ' in the matrix of F using optical microscopy. The fraction of the matrix phases ($\gamma+\gamma'$) in F and F_B is also greater than in E and E_B. This suggests that some of the β and β' have dissolved at the expense of γ and γ' as the fractions of the phases move towards their equilibrium values during the preheat and extrusion. The boron doped materials, E_B and F_B, show no significant differences optically when compared with the boron free materials.

COMPRESSION TESTS

Typical plots of the room temperature compressive stress *v.* strain for the new materials and MeMeC D (Ref. 6) tested in the transverse direction are shown in Fig. 3. The E_B specimen is slightly stronger than E but shows a similar strain to failure. The plots for neither E nor E_B differ significantly from that for D, either in terms of yield strength or strain to failure. In contrast, both F and F_B show a significant increase in strain to failure at room temperature with a maximum failure strain of 33% recorded for F_B.

The variation with temperature of the compressive yield strength and the compressive strain to failure in the transverse direction are shown in Fig. 4. In all cases, the elastic strain was subtracted to give only the plastic strain to failure. The curves for D and E_B show similar behaviour across the whole temperature range, although that for E_B appears to show that this material retains its yield strength better at higher temperatures. Composite E shows a lower yield strength but slightly greater strain to failure at temperatures up to 650°C. Above this temperature the yield strength of E starts to approach that of E_B, exceeding that of D. In all three materials, the strain to failure and yield strength remain approximately constant up to 500°C above which temperature the strength falls and the strain to failure rises.

As already noted, F and F_B show significantly higher room temperature strain to failure. This is reduced at 300°C

Table 3 Intensities of (100) and (110) γ' superlattice reflections relative to that of (200) reflection to which both γ and γ' contribute

Powder	Intensity (100)/(200), %	Intensity (110)/(200), %
Old γ'	5·4	6·2
New γ'	6·2	4·5
$\gamma+\gamma'$	2·9	2·9

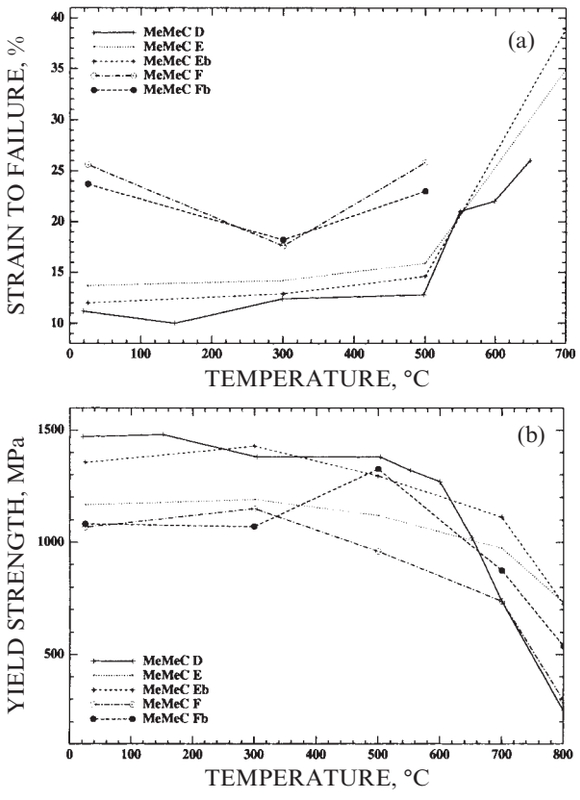

a compressive strain to failure; *b* compressive yield stress

4 Variation of given property with temperature

in both variants, although still exceeds that of the other MeMeC materials. At 500°C the strain to failure increases once more and is comparable with the room temperature value. Above 500°C compressive failure did not occur in F and F_B, i.e. specimens were deformed until almost completely flat. The yield strengths of F and F_B are both slightly less than that of the other variants at room temperature, although still in excess of 1000 MPa. As the temperature is increased the variation in the yield strength of F is similar to the other MeMeC materials, in that it remains approximately constant and then begins to fall at the highest temperatures. In contrast, F_B shows a peak in its compressive yield strength between 500°C and 700°C. This peak is the result of the behaviour of the γ' phase which is well known to exhibit a rise then fall in strength with increasing temperature. A peak in strength of γ' is expected at $\sim$700°C.[11] It is notable that F, which has a similar fraction of γ' does not show this behaviour. This may be because plastic yielding of the matrix is a more dominant deformation mechanism in F_B than in F, where brittle failure is more prevalent (*see* the subsection below on 'Fractography').

TENSILE TESTS

The average failure strengths of the MeMeC materials tested in tension are shown in Fig. 5*a*. In all cases, tensile failure occurred by fracture before yielding. Nevertheless, the fracture strength was greatly increased by the presence of boron and γ in the matrix. For example, the average fracture strength of F_B was 833 MPa compared with a value of 435 MPa for E. It can be seen that, in tension, boron has a more significant effect on the fracture strength of both E and F than it has on the strength in compression. This is not surprising since boron is expected to act by enhancing the grain boundary cohesion which will have a greater influence on the tensile properties. It was quite remarkable that the

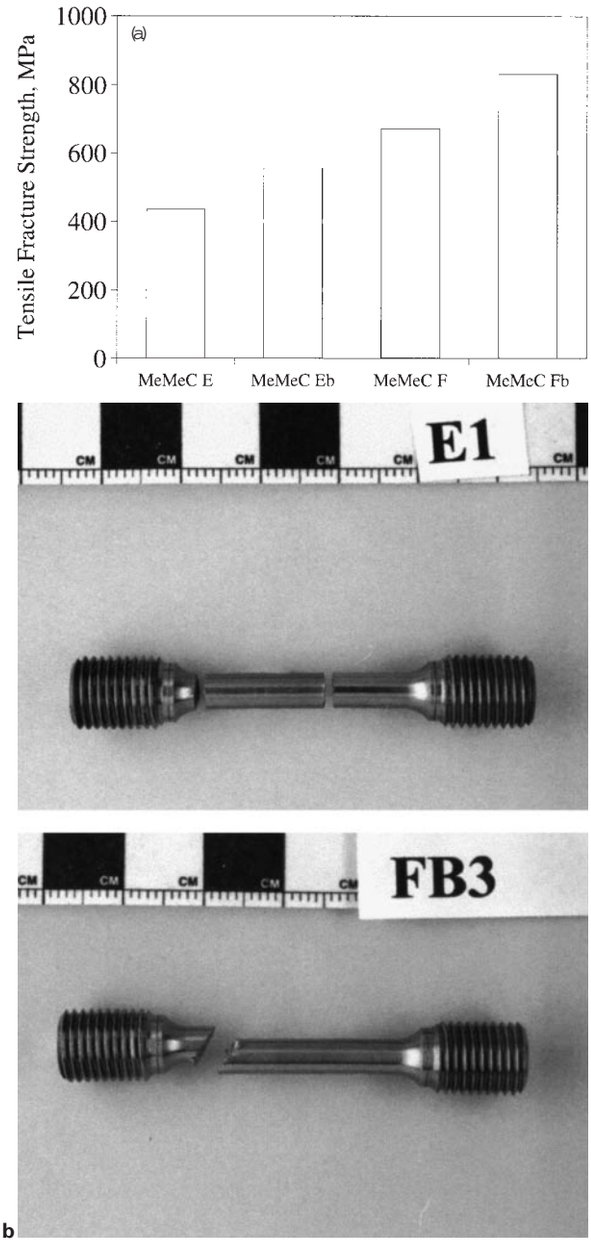

5 *a* tensile fracture strength results; *b* typical examples of failed MeMeC E and MeMeC F_B specimens

fracture surfaces of failed specimens of F_B were always inclined to the tensile axis, presenting a shear mode of failure as opposed to those of E, E_B, and F which were normal to the tensile axis (Fig. 5*b*). This demonstrates a more ductile failure mode for F_B compared with the other variants. Whereas F_B specimens always failed within the gauge length to give valid tensile tests, all the other specimens exhibited brittle characteristics with the first fracture event causing a further scission along the gauge length as a result of the shock of failure. The latter tensile specimens were therefore always in three pieces following testing. The results for F_B are therefore extremely encouraging and demonstrate the alloy design concepts used to enhance ductility.

FRACTOGRAPHY

Figure 6 shows two SEM fractographs with Fig. 6*a* showing the fracture surface after tensile failure of E_B. Similar fracture surfaces were also observed for E and F.

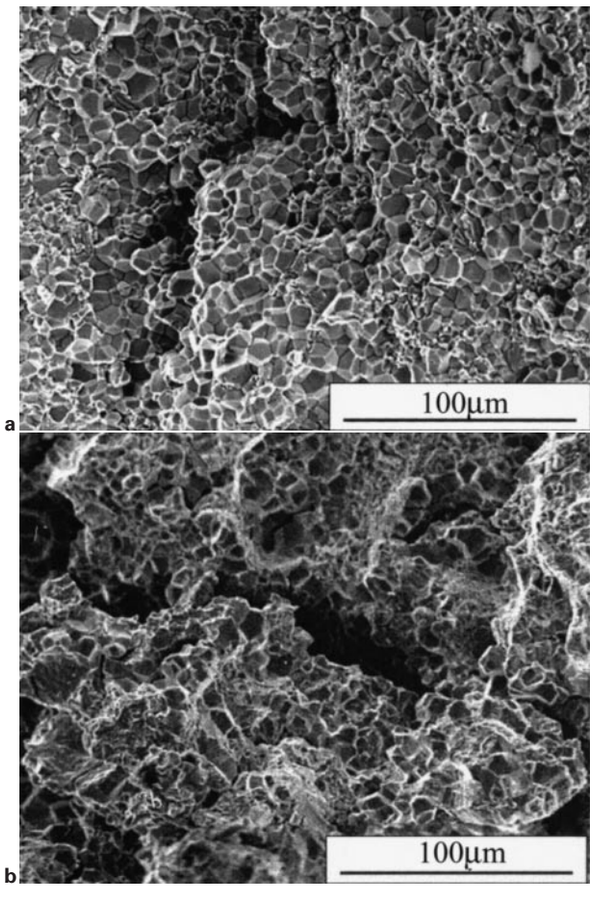

a MeMeC E_B; *b* MeMeC F_B

6 Fracture surfaces of given materials after tensile failure

This type of fracture surface is characteristic of brittle failure. The surface is planar, individual grains are easily recognised, and the failure has occurred by intergranular crack propagation. In contrast Fig. 6*b* shows a far more irregular fracture surface, found to be characteristic of F_B. Examples of both transgranular and intergranular fracture can be observed. The increased tensile fracture strength is undoubtedly attributable to this change in fracture mode due to the strengthening of grain boundaries by boron and because of the presence of the γ phase in the microstructure.

Conclusions

A variety of metal–metal composite materials based on the Ni–Al–Ti system have been manufactured, mechanically tested, and examined. The production route allows the initial composition of either the matrix (γ', $\gamma+\gamma'$) or reinforcement (β, β') to be modified independently. In this study, various matrix compositions were chosen to give (a) a γ' matrix containing >25 at.-%Ni either with or without boron additions and (b) a $\gamma'+\gamma$ matrix, again either with or without boron. The following conclusions have been drawn.

1. The mechanical properties of MeMeC E (which has a Ni rich γ' matrix) and E_B (with the same matrix, boron doped) are comparable to those of MeMeC materials produced in previous studies. In contrast, F and F_B which have a matrix sufficiently high in nickel to contain γ show a dramatic increase in compressive strain to failure (which is approximately doubled at room temperature) compared with the other MeMeC variants. This increase in strain to failure is not accompanied by a similar reduction in yield strength (in both F and F_B a room temperature compressive yield strength in excess of 1000 MPa is retained).

2. Materials E and the boron containing E_B show similar compressive mechanical properties. Boron additions also do not make a significant difference to the compressive behaviour of F, except at $\sim 500^\circ$C where the boron containing F_B shows a peak in strength which is not exhibited by F. The main role of boron is to enhance grain boundary cohesion in the matrix and thus suppress intergranular fracture. The compressive stress acting on the majority of the grain boundary area during testing will itself reduce the tendency for this failure mode, and thus any effect of boron is likely to be masked in compression.

3. All MeMeC materials tested in tension fail by fracture before general plastic yielding. Nevertheless, the tensile fracture strength is greatly improved by the presence of boron and γ within the matrix, with F_B showing the highest fracture strength (833 MPa). Boron additions improve the tensile fracture strength of both E and F by ~ 150 MPa, the most likely mechanism for this being an enhancement of the grain boundary cohesion in the matrix.

4. Fractography of specimens after failure in tension reveals that the failure mode in F_B is markedly different from that of all the other variants. E, E_B, and F exhibit planar fracture surfaces which are perpendicular to the tensile axis and failure occurs by intergranular fracture. In contrast F_B shows a much more irregular fracture surface, inclined to the tensile axis. Failure occurs by a combination of transgranular and intergranular fracture. This change in fracture mode may explain the substantial improvement in tensile fracture strength exhibited by F_B.

Acknowledgements

The authors are grateful to the Defence Evaluation and Research Agency, UK and the Civil Aviation Research and Development programme for funding this work. They would also like to thank Mike Henderson, Neil Jones, John O'Driscol, and David Knowles for helpful discussions.

References

1. A. MISRA and R. GIBALA: *Metall. Trans. A*, 1997, **28A**, 795.
2. J. D. WHITTENBERGER, R. D. NOEBE, D. R. JOHNSON, and B. F. OLIVER: *Intermetallics*, 1997, **5**, 173.
3. A. MISRA, Z. L. WU, M. T. KUSH, and R. GIBALA: *Philos. Mag. A*, 1998, **78**, 533.
4. D. R. JOHNSON, B. F. OLIVER, R. D. NOEBE, and J. D. WHITTENBERGER: *Intermetallics*, 1995, **3**, 493.
5. L. C. HSUING and H. K. D. H. BHADESHIA: *Metall. Trans. A*, 1995, **26A**, 1895.
6. J. D. ROBSON and H. K. D. H. BHADESHIA: *Mater. Sci. Technol.*, 2000, **16**, 349.
7. R. DAROLIA: *J. Met.*, 1991, **43**, 44.
8. M. YAMAGUCHI, Y. UMAKOSHI, and T. TAMANE: *Philos. Mag. A*, 1984, **50**, 205.
9. C. T. LUI, C. L. WHITE, and J. A. HORTON: *Acta Metall. Mater.*, 1990, **38**, 561.
10. R. YANG, N. SAUNDERS, J. A. LEAKE, and R. W. CAHN: *Acta Metall. Mater.*, 1992, **40**, 1553.
11. N. S. STOLOFF: *Int. Mater. Rev.*, 1989, **34**, 153.